



Removal of cationic dyes from aqueous solutions using adsorbents based on GO/APTG nanocomposites

Hui Xu*, Yajuan Zhang, Jin Tang, Weiguo Tian, Zeting Zhao, Yong Chen*

College of Petrochemical Technology, Lanzhou University of Technology, Lanzhou, China, Tel. +86-931-2975872; emails: xuhui@lut.cn (H. Xu), chenylut@126.com (Y. Chen), 1799797925@qq.com (Y.J. Zhang), 122493279@qq.com (J. Tang), 3047007413@qq.com (W.G. Tian), 742801123@qq.com (Z.T. Zhao)

Received 9 March 2019; Accepted 12 September 2019

ABSTRACT

In the present study, the cheap and naturally available one-dimensional modified attapulgite (APTG) with hexadecyl trimethyl ammonium bromide (CTAB) was introduced to synthesize graphene oxide (GO)/APTG composites and used as adsorbent to remove two cationic dyes, methylene blue (MB) and rhodamine B (RhB) from aqueous solution in single and binary dye systems. The structure and morphology of the GO/APTG composites were characterized by Zeta, Fourier-transform infrared spectroscopy, scanning electron microscopy and transmission electron microscopy and Brunauer–Emmett–Teller. The GO/APTG exhibits good adsorption performance for MB, RhB as well as the other cationic dyes in single systems, and has a significant improvement compared with APTG. However, in a binary dye system, the adsorption performance of MB was significantly better than that of RhB due to the rival adsorption. Removal mechanism suggests that electrostatic attractions and π - π stacking play essential roles. Additionally, the molecule structures of dyes exert a certain influence on the removal process. The adsorption kinetics and isotherm studies at different temperatures of GO/APTG in single as well as binary dye systems revealed that adsorption process was fitted well with the pseudo-second-order model and Langmuir adsorption isotherm showed the best compatibility with the experimental data in comparison with other isotherm models, the maximum adsorption capacity of MB and RhB can be 534.76 and 473.93 mg g⁻¹ in a single system; respectively, which were high adsorption performances. For its advantages of easy preparation, low cost and excellent adsorption performances, GO/APTG could be an eco-friendly and promising adsorbent for the removal of organic cationic dyes from wastewaters.

Keywords: Attapulgite; Graphene; Surface modification; Binary dye system; Cationic dye removal

1. Introduction

In recent years, with the rapid development of many industries (printing, textile, paper, and plastics), a considerable amount of dye wastewaters was discharged into the aquatic environment [1]. Compared to anionic dyes, the cationic dyes methylene blue (MB) and rhodamine B (RhB) is carcinogenic, genotoxic, mutagenic, and teratogenic due to their synthetic origin and aromatic ring structure with delocalized electrons. The dyes were emitted directly into

the river that will generate great harmful to the aquatic environment, human body, social stability and economic development [2–5]. Therefore, the various technologies of control water pollution, such as adsorption, coagulation, extraction, and chemical oxidation have been developed to treat dye wastewater. In many ways, the adsorption method is more promising than other available water treatment techniques for the removal of dyes from aqueous solutions, due to its flexible, more convenient, simple of design, clean, effective

* Corresponding authors.

and economical method [1,6]. Therefore, the development of novel and cost-effective adsorbents to remove organic dyes has been one of the most active study efforts in wastewater treatment.

Recently, graphene and its derivatives have attracted wide interests as effective adsorbents for pollutants removal from the environment due to their unique lamellar structure and physicochemical properties. The graphene-based material not only provides a large specific surface area, which can form strong interactions with to remove contaminants but also possesses affinity towards several of organic pollutants. In recent years, there are lots of applications of graphene-based materials in adsorbents that have been carried out by researchers [7]. However, graphene nanosheets often suffer from serious agglomeration or re-stacking due to Van der Waal's interaction. And graphene-based adsorbents are relatively expensive, which may be ineffective in adsorption of organic pollutants and hinder the wider application of graphene-based adsorbents. Consequently, it is necessary for practical applications that combination of low-cost adsorbents and high absorbability of graphene. The use of clay materials represents an economical and environmentally friendly approach in modifying graphene oxide (GO) for environmental applications such as organic dyes adsorption [8].

The clay mineral attapulgite (APT), a form of magnesium aluminum silicate mineral, has advantages of unique one-dimensional structures, high surface specific area, and good cation exchange capacity compared with other clay minerals [9,10]. Attapulgite is widely used as a low-cost adsorbent for the removal of metal ions and organic pollutants [11,12]. Despite the comparative low-cost of APT, APT exhibits poor performances such as long adsorption time, low adsorption efficiency and badly usability when pH is not adjusted in pollutant adsorption. A feasible solution is to use a stable substrate with the abundant active sites to load clay nanomaterial to increase its adsorption efficiency [13]. GO as a derivative of graphene it contains a large number of oxygen-containing functional groups, such as carboxyl ($-\text{COOH}$), hydroxyl ($-\text{OH}$), carbonyl ($-\text{C}=\text{O}$), reacting with dye ions through electrostatic interaction and π - π stacking [14,15]. This study reports for the GO composite with APT removal organic dyes in solution. GO was synthesized using Hummers and Offeman [16] method for this purpose.

At present, the coexistence of various dyes in industrial wastewater is a serious environmental problem. Thus, the simultaneous removal of multiple organic dyes from wastewater has a particular significance to both pollution control and remediation. And as per the best of our knowledge, no such research has been reported in the existing literature for the removal of MB and RhB in single as well as a binary system. In this paper, to enhance the adsorption performances of the natural clay mineral APT, APT modified with a cationic surfactant hexadecyl trimethyl ammonium bromide (CTAB) can be combined with negatively charged GO through electrostatic attraction, the surface of the GO/attapulgite/cetyltrimethyl ammonium bromide (APTG) composite with negatively charged can easily adsorb positively charged cationic dyes. The interaction between the adsorbent and the adsorbate is important in the adsorption process. The study explores the possible interaction for the

removal of cationic dyes using GO/APTG and understanding its removal mechanism. A series of experiments such as GO and APTG different mass ratios, effects of contact time, pH, initial dye concentration, adsorbent dose, and temperature on the adsorption were investigated. Also, the removal performance for other types of dyes on GO/APTG has been assessed. The results indicated that the removal efficiency of cationic dyes was superior to that of anionic dyes (Alizarin Yellow R (AYR), Orange Yellow IV (Orange IV)). It is attributed to the electrostatic attraction that the GO/APTG is negatively charged. The kinetics, isotherms of dyes, and thermodynamic studies were also performed to study the adsorption mechanism and interactions among the dyes and adsorbents. The studies demonstrated that GO/APTG was beneficial to the removal of cationic dyes and might use as a low-cost and eco-friendly adsorbent for the removal of dyes from wastewaters.

2. Experimental details

2.1. Materials

Attapulgite was obtained from Jiangsu Province, China. Natural graphite flakes potassium concentrated sulphuric acid (H_2SO_4 , 98%), permanganate (KMnO_4), hydrogen peroxide (H_2O_2), hydrochloric acid (HCl), sodium hydroxide (NaOH), and CTAB were analytical grade reagent. MB, RhB, Orange IV, AYR, Basic Fuchsin (BF) and Crystal violet (CV) were selected for this study, they were used without any additional purification and their relative molecular mass, λ_{max} and structure are shown in Table 1.

2.2. Preparation of GO/APTG

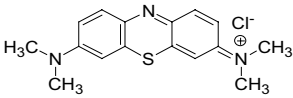
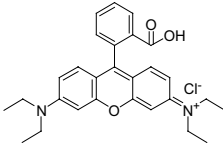
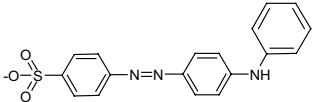
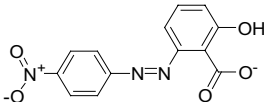
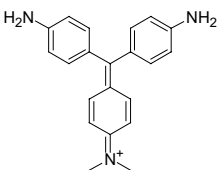
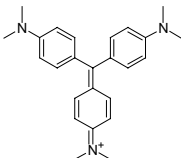
0.656g CTAB (CTAB is an abbreviation for cetyltrimethylammonium bromide. The chemical formula is $\text{C}_{16}\text{H}_{33}(\text{CH}_3)_3\text{NBr}$) was introduced into 100 mL 100 g L^{-1} APT suspension under electromagnetic stirring for 12 h. The solid was filtered, washed and then dried in vacuum at 60°C for 24 h to obtain the grafted of APT, which was named APTG. And GO was synthesized by the modified Hummers and Offeman method [16].

0.3 g L^{-1} GO aqueous suspension was slowly added into 0.3 g L^{-1} APTG aqueous suspension under mild electromagnetic stirring. And then the suspension was treated to sonication for 30 min. Several drops of dilute HCl solution were added to the reaction mixture until the pH value was adjusted to 2. With the addition of dilute HCl, brown floccule gradually appeared and deposited at the bottom of the reaction mixture. The derived products were filtrated and washed thoroughly with distilled water, and then the resulting GO/APTG was dried in an oven at 60°C.

2.3. Characterization

Fourier-transform infrared spectroscopy (FTIR) concerning composite materials was determined to employ FTIR (NEXQS670, America) using KBr pellets. Morphology and structure of composite materials were observed by scanning electron microscopy (SEM, JSM-6701F, and Japan) and transmission electron microscopy (TEM, JEM-1200EX, America). Zeta potential (Malvern Instruments Zetasizer Nano-ZS) was obtained at room temperature. The N_2 adsorption-desorption,

Table 1
General characteristic of the studied dyes

Name	Molecular weight	λ_{\max} (nm)	Structure
Methylene blue (MB)	319.9	664	
Rhodamine B (RhB)	479.0	552	
Orange IV	375.4	444	
Alizarin Yellow R (AYR)	287.2	373	
Basic Fuchsin (BF)	347.4	540	
Crystal violet (CV)	407.9	590	

specific surface area and pore size distribution of the sample were analyzed by American ASAP 2020 plus HD88 specific surface area and porosity analyzer, using the Barrett–Joyner–Halenda (BJH) method, respectively.

2.4. Batch adsorption experiments

100 mg L⁻¹ of dye solution (single and binary dye systems of MB or RhB) 60 mL and 0.02 g of adsorbents were added in the 250 mL conical flask, which was immediately sealed and solution pH was adjusted to the desired value by the micro-scale of HCl and NaOH. The mixed solution was stirred with 300 rpm for 250 min at 303 K. After adsorption, they were filtered through 0.45 μm membranes and measure the residual concentration of dye. The removal capacity and the removal efficiency of dye were calculated using the following equations:

$$q_B = \frac{C_0 - C_e}{m} \times V \quad (1)$$

$$R = \frac{C_0 - C_e}{C_0} \times 100\% \quad (2)$$

where C_0 and C_e are the initial and equilibrium concentrations of dye in solution (mg L⁻¹), V is the volume of solution (L); m is the mass of adsorbent (g).

2.5. Determination of two-component dyes

In general, the concentration and absorption values were determined in single dye at their λ_{\max} , but for two-component dyes, where is a large spectral interference (absorption bands overlap), readings at a single dye's λ_{\max} may cause inexact results. The simultaneous solution of the equations helps to solve the problems of spectral overlapping. For binary dye systems, the concentration of dye was measured using a UV-Spectrophotometer (7230G, China) at two wavelengths of 664 and 552 nm, respectively. The dye concentrations in solutions were determined by the following equations [17]:

$$C_A = \frac{k_{B2}A_1 - k_{B1}A_2}{k_{A1}k_{B2} - k_{A2}k_{B1}} \quad (3)$$

$$C_B = \frac{k_{A1}A_2 - k_{A2}A_1}{k_{A1}k_{B2} - k_{A2}k_{B1}} \quad (4)$$

where C_A and C_B are the concentrations of components A and B in solution; k_{A1} , k_{A2} , k_{B1} and k_{B2} are the calibration constants for components A and B at wavelength λ_1 and λ_2 , respectively; A_1 and A_2 are the absorbances at wavelength λ_1 and λ_2 .

3. Results and discussion

3.1. Characterization

The zeta potential experiments of GO, APTG and GO/APTG under different pH values are shown in Fig. 1 to determine their surface charges. Commonly, the outer surfaces of APT and GO with negatively charged [18,19], which makes them unable to be combined through electrostatic attraction. CTAB, a cationic surfactant, has been chosen to modify APT, which leads to getting APTG with the outer surface positively charged. When the pH value comes to 2, the zeta potential of GO and APTG are -25.9 and 12 mV, respectively, which made the potential difference between APTG and GO is largest, which is more favorable to combining closely of GO and APTG by electrostatic attraction. The observed pH of the zero point charge for GO/APTG composite was found to be 2 (Fig. 1). That means at pH 2, there will be a net-zero charge on the surface and below this pH, a net positive charge will be there and above this pH, a net negative charge will be there on the surface of the adsorbent [20]. Such behavior is beneficial for removing cationic dyes.

Fig. 2 reveals the FTIR spectra of adsorbent APT, APTG, GO, GO/APTG composites. We can gain the new peaks appearing at $2,925$ and $2,860$ cm^{-1} are the stretching vibrations of methyl group ($-\text{CH}_3$) and methylene ($-\text{CH}_2-$) [21], respectively, in addition to this, the peaks of APTG and APT are basically consistent, which proves CTAB not damage the functional groups of APT and organic groups of CTAB have been combined with the surface of APT that corresponded to the result of the zeta potential analyzed. The strong bands at $3,418$ and weak bands at $1,730$; $1,625$; $1,400$; $1,220$; and $1,047$ cm^{-1} of GO separately assign to the stretching vibration of $-\text{OH}$ groups in water molecules, the $\text{C}=\text{O}$ stretching vibration of the carboxylic acid groups, the vibration of aromatic $\text{C}=\text{C}$ groups, the $-\text{OH}$ stretching vibration of the carboxylic

acid group, the vibration of epoxy $\text{C}-\text{O}-\text{C}$ groups, the $\text{C}-\text{O}$ vibration of various oxygen-containing groups [22]. It can be indicated that GO has been formed through oxidizing graphite, and the surface has been distributed to different kinds of oxygen-containing functional groups. The FTIR spectra of GO/APTG composites contain both the peaks of GO and the peaks of APTG, indicated a combination complete between the modified APTG and GO.

To better understand morphology GO and GO/APTG, the SEM and TEM images are presented in Fig. 3. The images can be seen as the laminated structure of GO and the rod-like structure of APTG, which means that the synthesis of composite material did not significantly change the morphology of GO and APTG. And APTG uniformly dispersed and intercalated the surface of GO and between the GO films, indicating that the combination between APTG and GO has been well completed, which was by the FTIR analyzed. Furthermore the wrinkled and folded regions less composite material of GO/APTG than GO, showing the APTG added can reduce to the stacking of GO to some degree [23].

Fig. 4 shows the N_2 adsorption–desorption isotherm and pore size distribution curve of GO/APTG that is a typical type II adsorption isotherm, indicating that GO/APTG has mesopores ($2-50$ nm) and macropores (>50 nm), and appears hysteresis loop H_3 [24]. The mesoporous structure and high specific surface area promote the reaction of the composite with the dye molecules, thereby increasing the dye removal rate. The Brunauer–Emmett–Teller surface area of the GO/APTG is 33.88 m^2 g^{-1} and the BJH adsorption cumulative volume of pores is 0.070 m^3 g^{-1} .

3.2. Adsorption of dyes

3.2.1. Effect of different materials on dye adsorption

Fig. 5 displays the adsorption of MB (RhB) on APT, APTG, GO, GO/APTG against time in single dye solutions. The adsorption capacity of APTG for MB and RhB is respectively 62.07% and 23.98% that was lower than APT of 64.22% and 32.12% . Due to MB and RhB are cationic dyes and APTG with a positive charge on the surface, leading to declined adsorption on APTG. The phenomenon also

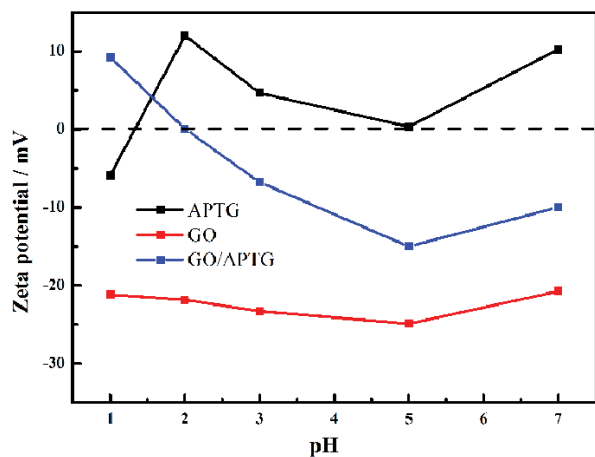


Fig. 1. Zeta potential experiments of GO, APTG and GO/APTG.

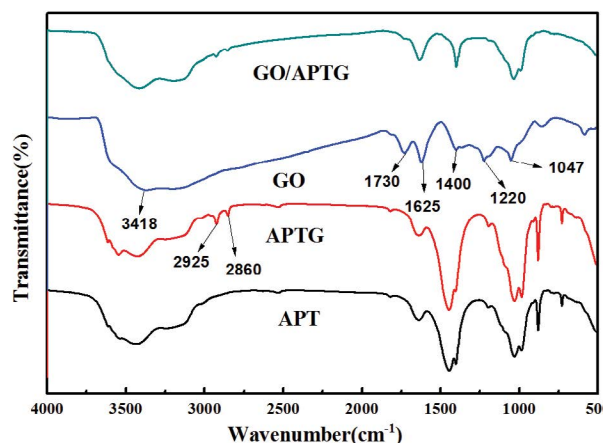


Fig. 2. FTIR of APT, APTG, GO, GO/APTG.

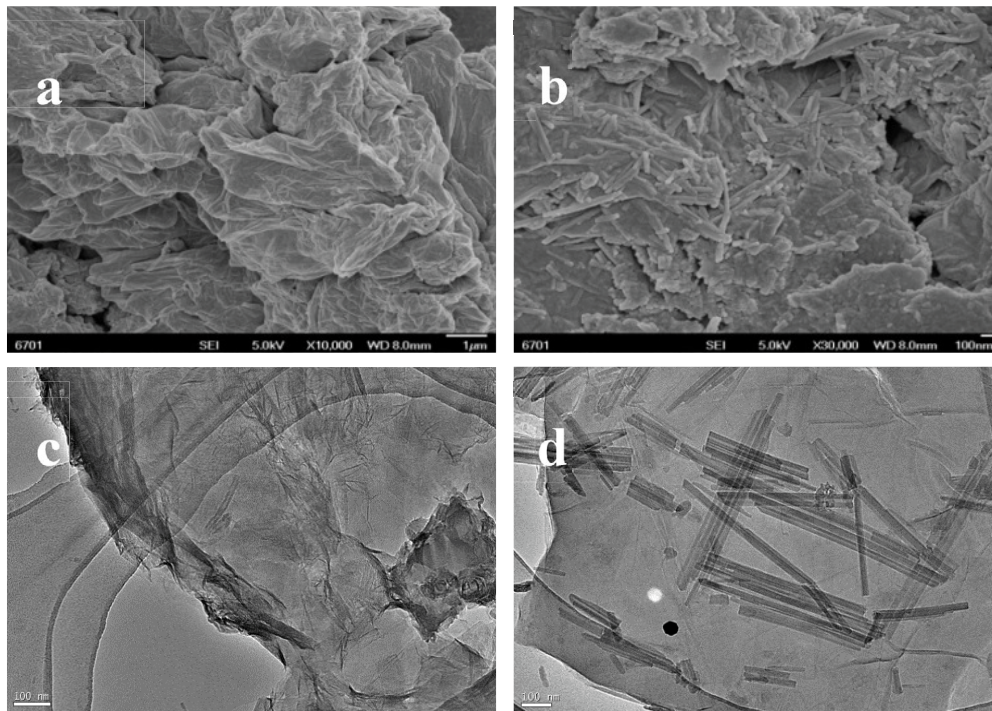


Fig. 3. SEM images of (a) GO and (b) GO/APTG; TEM images of (c) GO, and (d) GO/APTG.

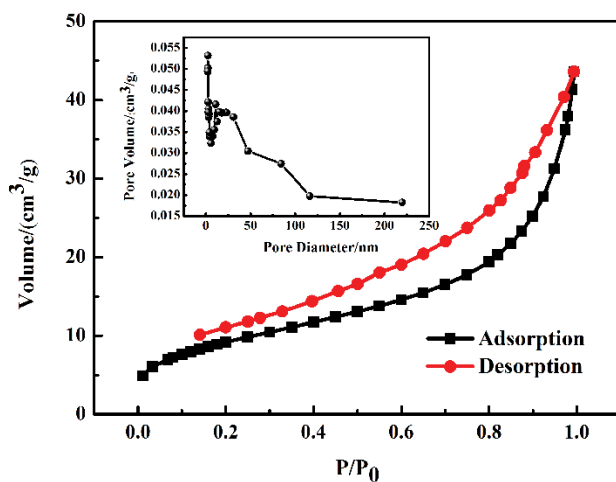


Fig. 4. N_2 adsorption-desorption isotherms and pore size distribution of GO/APTG composite.

proves that APT has been successfully modified. When the APT was modified with a cationic surfactant CTAB, it can be combined with negatively charged GO through electrostatic attraction. The adsorption property for cationic dyes can significantly enhance. It is mainly attributed to that the surface of the GO/APTG composite with negatively charged can easily adsorb positively charged cationic dyes. It can be observed that when the mass ratio of GO to APTG is 1:1, the adsorption effect is the best and the dye adsorption showed a fast adsorption equilibrium at 60 min. The adsorption capacity of MB was as high as 293 mg g^{-1} , the adsorption rate reached 97.7% that equal to the adsorption effect of GO that

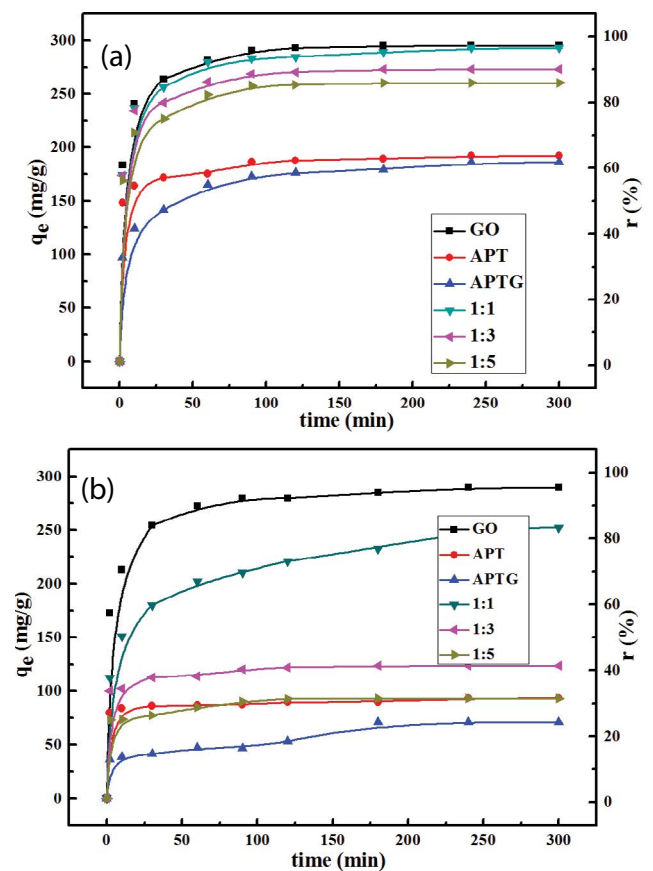


Fig. 5. Adsorption of (a) MB and (b) RhB on APT, APTG, GO, GO/APTG (1:1, 1:3, 1:5) in single-dye solutions.

the adsorption rate was 98%. For RhB was 252 mg g⁻¹, the adsorption efficiency was 84% that lower than the removal rate of GO was 96%. Weng et al. [25] researched RGO/Fe NPs as an adsorbent removed MB that the maximum adsorption capacity is 199.4 mg g⁻¹. Also, Cheng et al. [26] applied to GO modified zeolite made the composite material graphene oxide/beta zeolite (GB) to remove RhB that maximum adsorption capacity is only 64.47 mg g⁻¹. It shows that the GO/APTG exhibits good adsorption performance for both MB and RhB, and has a significant improvement compared with APTG. Although the removal rate of MB and RhB for GO/APTG is slightly lower than that of GO, considering the cost of the composite adsorbent decrease, GO/APTG may be used as a cost-effective adsorbent for organic dyes. In the subsequent studies, the mass ratio of GO to APTG was 1:1.

3.2.2. Effect of pH in binary-dye solutions

The initial value pH of the solution not only has a significant effect on the color of dye in water but also is one of the most important factors that affect on adsorption property of composite materials [27]. The study results were shown in Fig. 6 and the composite GO/APTG has a better adsorption effect on MB and RhB in the range of pH value was 5–7. It can be seen that the adsorption capacity and removal efficiency of MB has greatly enhanced as the increase of value pH in binary-dye systems, which changed trend was by the single-dye systems. It is indicated that with the augment of the pH, the electrostatic attraction between the GO/APTG composite and cationic dyes increases, helping to remove cationic dyes. The result is lined with the influence of pH on the zeta potential of the GO/APTG. Also, APT is protonated through the Si–O–Si of APT change to the Si–OH groups [28], which leads to an increase in the number of active sites. While, compared to MB, the adsorption capacity of RhB was descend that was opposite whether in single-dye or binary-dye systems. It is attributed to that GO in composite material plays a major role in the adsorption of RhB. The carboxyl group of RhB has a strong positive charge density at lower pH, leading to the electrostatic adsorption was enhanced between GO and RhB [29]. So, the adsorption capacity is the

highest when pH = 2 for RhB. With the value increase of pH, a large number of OH⁻ appearing in aqueous solutions was easier to combine with RhB, hindering RhB was adsorbed. So the composite materials adsorbing capacity of RhB was gradually decreasing.

3.2.3. Effect of adsorbent dosage in binary-dye solutions

The adsorbent dosage is one of the most important factors that affect adsorption property. The effect of adsorbent dosage on the removal efficiency of MB and RhB in a single system has been investigated. After 60 min, when the adsorbent dosage is 0.01, 0.02, 0.04, 0.06, and 0.08 g, the removal efficiencies of MB were 91.12%, 97.70%, 97.92%, 98.16%, 98.48% and the removal efficiencies of RhB were 77.32%, 84.1%, 84.51%, 85.02%, and 85.43%, respectively. Fig. 7 shows that the MB and RhB adsorption rate when the adsorbent dosage range of 0.01–0.08 g in binary-dye solutions. The adsorption rate of MB rapidly increased in the low dosage, while RhB was a moderate increase, which indicates the dominance of MB in the competition with RhB. When the adsorbent

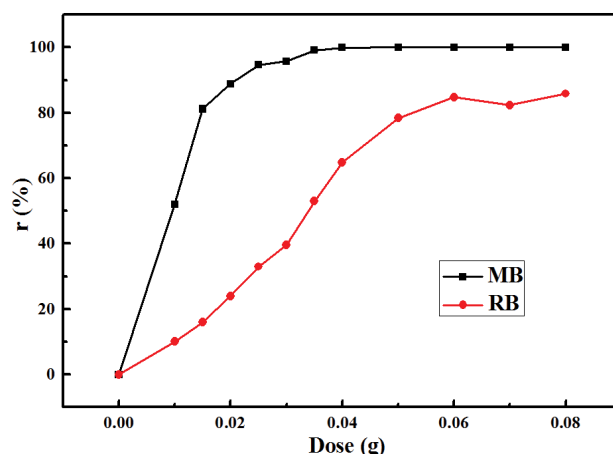


Fig. 7. The adsorbent dosage affects MB and RhB adsorption by GO/APTG in binary-dye solution.

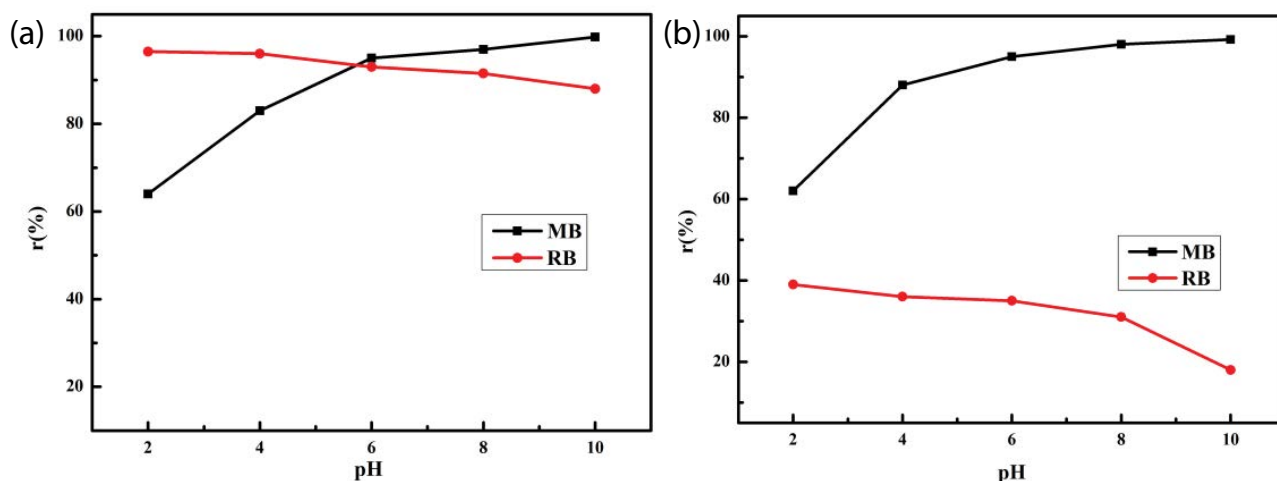


Fig. 6. Effect of pH on MB and RhB adsorbed by GO/APTG: (a) single-dye and (b) binary-dye solutions.

dosage was 0.02 g, the adsorption rates of MB and RhB were 82.9% and 23.9% in the binary-dye system. Compared to dual vs. unitary dye systems, the MB adsorption rate decreased slightly and RhB significantly, indicating that MB was true to be preferentially adsorbed. With adsorbent dosage increased, the adsorption rate of RhB started to increase after the adsorption equilibrium of MB quickly reached. This is owing to the available adsorption sites increased, which cause the rival adsorption between dyes decreased. The more the adsorbent, the higher the removal efficiency there are in a single or binary system. This is because more dosage means more adsorption active sites, which can capture more dye molecules. But more dosage will cause a decrease in the adsorption capacity. Therefore, taking into account adsorption capacity and for comparison, the optimum adsorbent dosage is 0.02 g.

The transport coefficient and the separation efficiency of the solute in the two phases are also represents using the partition coefficient K by Eq. (5). The selective adsorption partition coefficient by Eq. (6) of GO/APTG to MB and RhB was calculated using the following equation:

$$K_d = \frac{C_0 - C_f}{C_f} \times \frac{V}{m} \quad (5)$$

where K_d is the selective adsorption partition coefficient, C_0 and C_f are the initial and equilibrium concentrations of dye in solution (mg L^{-1}), V is the volume of solution (L), m is the mass of adsorbent (g).

$$k = \frac{K_d(T)}{K_d(I)} \quad (6)$$

where k is the selectivity coefficient, T represents MB and I represent RhB. The calculated results are shown in Table 2. It can be seen that GO/APTG composite exhibits higher selectivity for MB than RhB in binary-dye solutions and the degree of competition increases first and then decreases with the increased of dosage.

3.2.4. Effect of contact time and kinetic studies

The effects of different times on the adsorption properties of single-dye and binary-dye systems were studied. The results are shown in Fig. 8. It is apparent that the adsorption gradually increased for both systems with the contact time. The adsorption capacity of two dyes in the binary-dye system was lower compared with the single-dye system, whereas RhB decreased obviously. It is illustrated that there is rival adsorption between MB and RhB.

To further examine the adsorption mechanism of the adsorption process, the pseudo-first-order, the pseudo-second-order, and intra-particle diffusion kinetic models were applied to analyze the experimental data in single-dye and binary-dye systems. The linearized forms of the equations are respectively expressed by using Eqs. (7)–(9):

$$\ln(q_e - q_t) = \ln q_e - k_1 t \quad (7)$$

$$\frac{t}{q_t} = \frac{1}{k_2 q_e^2} + \frac{t}{q_e} \quad (8)$$

$$q_t = k_p \sqrt{t} + c \quad (9)$$

Table 2
Competitive binding behaviors of GO/APTG for MB and RhB

$m \text{ g}^{-1}$	$K_d (10^3 \text{ L kg}^{-1})$		k
	MB	RhB	
0.01	6.50	0.67	9.67
0.02	25.82	0.93	27.82
0.03	114.84	1.31	87.96
0.04	5,343.90	2.77	1,928.31
0.05	5,998.80	4.34	1,380.80
0.06	4,999.00	5.57	897.94
0.08	3,749.25	4.55	824.42

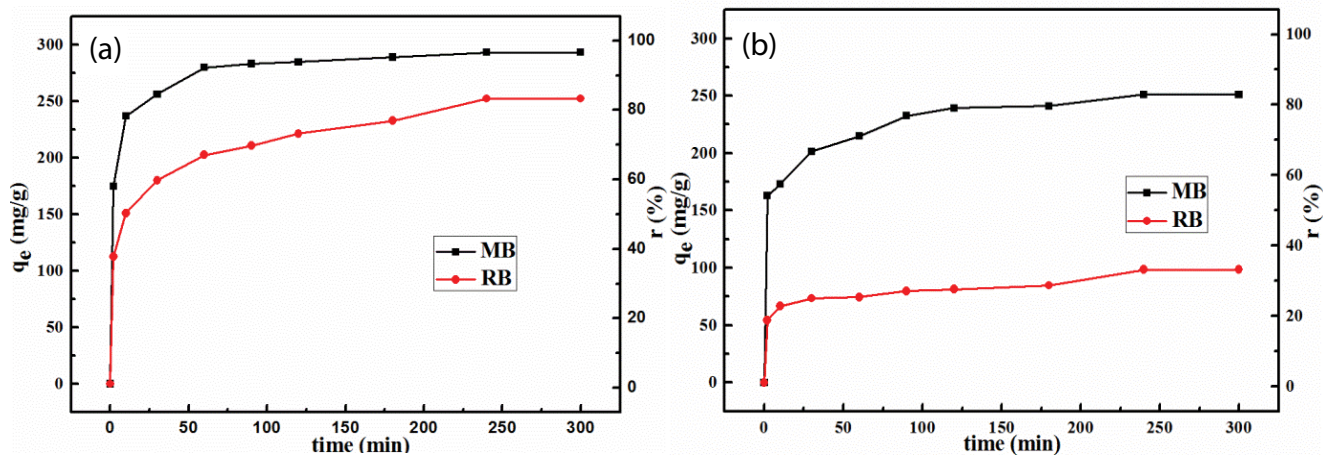


Fig. 8. Contact time was an effect on MB and RhB adsorbed by GO/APTG (1:1) in single-dye and binary-dye solutions.

where k_1 is the rate constant of pseudo-first-order model adsorption (min^{-1}), k_2 is the rate constant of pseudo-second-order model adsorption ($\text{g mg}^{-1} \text{min}^{-1}$), q_e is the adsorption capacity at equilibrium (mg g^{-1}), q_t is the adsorption capacity at time t (mg g^{-1}), t is contact time (min), k_p is the rate constant of intra-particle diffusion kinetic models ($\text{mg (g min}^{1/2})^{-1}$) and C is constant. The values of kinetic parameters are listed in Table 3.

The result shows that the R^2 of the linear pseudo-second-order model greater than 0.99 and the value of experimental q_e is in accordance with a fitting parameter of pseudo-second-order q_e (Table 3), which illustrates the adsorption of MB and RhB onto GO/APTG in single-dye or binary-dye system more in line with the pseudo-second-order kinetic model. Meanwhile, from the parameters of the pseudo-second-order kinetic model seen, the number of q_e in the binary-dye system were less than in single-dye system, for RhB is particularly evident, suggesting there is a rival adsorption in binary-dye systems, compared to RhB, MB more preferentially adsorbed on the GO/APTG.

While the R^2 of the linear intra-particle diffusion kinetic model is very low in two systems, the intra-particle diffusion kinetic model is not entirely suitable for describing the adsorption process, and this process should be controlled by the interlayer diffusion and film diffusion model. Thus, the adsorption process is divided into three parts: (1) the external surface adsorption. Dye molecules from the solution diffuse to the surface of the adsorbent of GO/APTG, showing a rapid adsorption process, (2) the slow adsorption. It is attributed to interlayer diffusion which is rate-controlled step, and (3) the adsorption equilibrium. Also, compared to the k_p values of MB and RhB can be seen, the diffusion rates of MB are greater than those of RhB, which suggests that GO/APTG has a higher affinity to MB especially in the binary-dye system.

3.2.5. Adsorption isotherms

For a better description of the interaction between MB (and RhB) and GO/APTG composites at different time (293, 313, and 333 K), different initial concentrations ($50\text{--}300 \text{ mg L}^{-1}$) and the amount of adsorbent was 20 mg in single-dye solution and binary-dye solution, MB and RhB adsorption equilibrium concentration and the relationship between adsorption capacities are respectively shown in Figs. 9 and 10. Moreover, the Langmuir, Freundlich, Tempkin, and Dubinin–Radushkevich (D-R) isotherms models are utilized to fit the experimental data. The equations are as follows:

$$\frac{C_e}{q_e} = \frac{C_e}{q_m} + \frac{1}{q_m b} \tag{10}$$

$$\ln q_e = \ln K_f + \frac{1}{n} \ln C_e \tag{11}$$

$$q_e = \beta \ln K_t + \beta \ln C_e \tag{12}$$

$$\ln q_e = \ln Q_s - B \epsilon^2 \tag{13}$$

where q_m is the calculated adsorption capacity at maximum (mg g^{-1}), q_e is the experimental adsorption capacity at equilibrium (mg g^{-1}), C_e is the equilibrium concentration of the solution (mg L^{-1}), b is a Langmuir constant (L mg^{-1}), K_f is a Freundlich constant (mg L^{-1}), $\beta = RT/b$, T is the absolute temperature in Kelvin, R the universal gas constant ($8.314 \text{ JK}^{-1} \text{ mol}^{-1}$), K_t the equilibrium binding constant, and the constant β is related to the heat of adsorption, B is a constant related to the adsorption energy, Q_s the theoretical saturation capacity (mg g^{-1}), $\epsilon = RT \ln(1 + 1/C_e)$ is the Polanyi potential (mol kJ^{-1}).

Another parameter R_L , a dimensionless equilibrium parameter, which is defined as follows:

$$R_L = \frac{1}{1 + k_L C_0} \tag{14}$$

where k_L is the Langmuir constant (L mg^{-1}) and C_0 is the initial concentration (mg L^{-1}).

Tables 4 and 5 summarize the calculated coefficients of determination (R^2) and model parameters of the Langmuir, Freundlich, Tempkin and D-R isotherms. As can be seen, that the linearly dependent coefficient R^2 of Langmuir model greater than 0.99 suggests that the isotherm data fit the Langmuir model, which indicates the adsorption processes of MB and RhB by GO/APTG belong to the monolayer adsorption manner in single-dye and binary-dye systems. From the Langmuir isothermal model fitting parameters, the maximum adsorption capacity of MB and RhB can be 534.76 and 473.93 mg g^{-1} in a single system; 534.76 and 168.92 mg g^{-1} in a binary system, respectively. Langmuir isolation factor (R_L) indicates the affinity of the adsorbent for the adsorbate. When this parameter indicates the isotherm is unfavorable ($R_L > 1$), favorable ($R_L < 1$), linear ($R_L = 1$), or irreversible ($R_L = 0$) [26]. Table 4 shows R_L values in the range of 0–1, which indicates the adsorption processed is favorable.

Table 3
Kinetic parameters for MB and RhB adsorption on GO/APTG

		Pseudo-first-order model			Pseudo-second-order model			Interlayer diffusion model	
		$k_1 \text{ min}^{-1}$	$q_e \text{ mg g}^{-1}$	R^2	$k_2 \times 10^{-3} \text{ g mg}^{-1} \text{ min}^{-1}$	$q_e \text{ mg g}^{-1}$	R^2	$k_p \text{ mg (g min}^{1/2})^{-1}$	R^2
Single system	MB	0.0172	66.84	0.8645	1.0074	295.86	0.9998	5.9915	0.6637
	RhB	0.0103	111.09	0.9437	0.3060	258.39	0.9949	8.2692	0.9214
Binary system	MB	0.0132	78.41	0.9199	0.5755	255.11	0.9988	5.7867	0.9012
	RhB	0.0070	31.17	0.8852	0.9180	95.79	0.9923	2.2884	0.9376

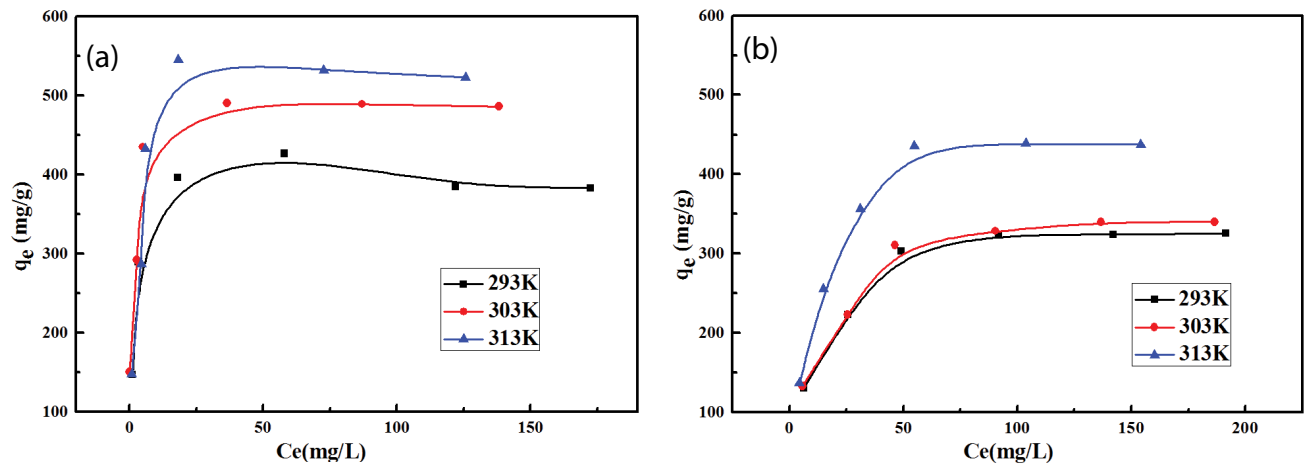


Fig. 9. Adsorption isotherms of MB (a) and RhB (b) in a single-dye solution.

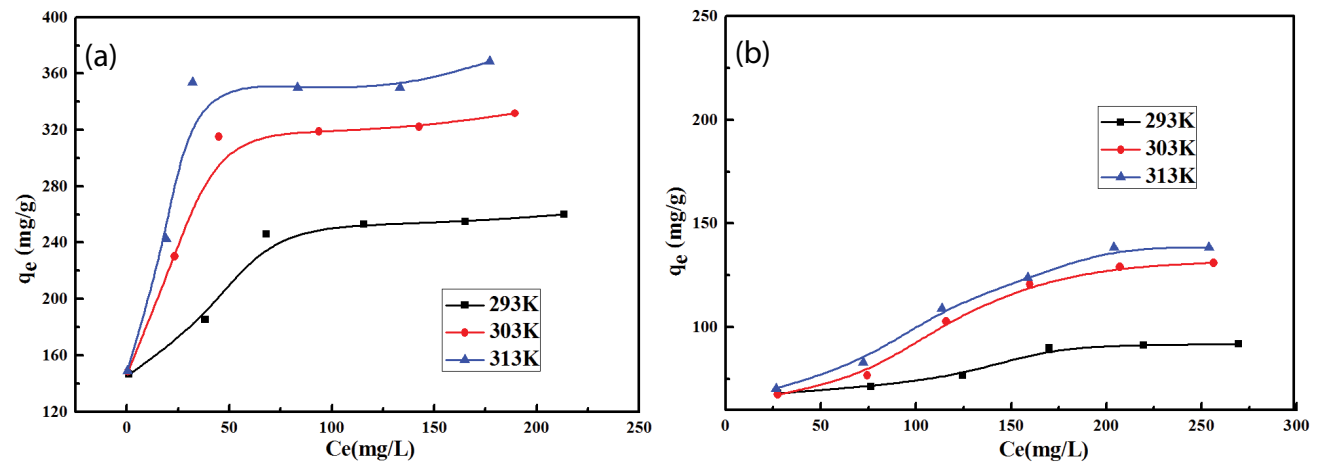


Fig. 10. Adsorption isotherms of MB (a) and RhB (b) in binary-dye solution.

Also, Table 6 summarizes the maximum adsorption capacity of different adsorbents reported in other literature for removing MB and RhB. It is worth noting that GO/APTG has higher adsorption capacity and shorter adsorption equilibrium time. Therefore, GO/APTG composites will be on track to apply in the wastewater treatment.

3.2.6. Thermodynamic study

The q_m of the Langmuir isotherm equation increased with the temperature increased. It is obvious that the higher the temperature, the higher the adsorption capacity, indicating that the adsorption process is an endothermic reaction, and the elevated temperature is favorable for the adsorption process. To study the effect of temperature on MB and RhB adsorbed by GO/APTG in single-dye and binary-dye solutions, the thermodynamic parameters such as Gibbs free energy (ΔG°), enthalpy (ΔH°) and entropy (ΔS°) are calculated by the following equations:

$$K_d = \frac{q_e}{C_e} \quad (15)$$

$$\Delta G^\circ = -RT \ln K_d \quad (16)$$

$$\ln K_d = \frac{\Delta S^\circ}{R} - \frac{\Delta H^\circ}{RT} \quad (17)$$

where q_e is the experimental adsorption capacity at equilibrium (mg g^{-1}), C_e is the equilibrium concentration of the solution (mg L^{-1}), R is the gas constant ($8.314 \text{ J mol}^{-1} \text{ K}^{-1}$), T is the absolute temperature (K) and K_d is the Langmuir constant (L g^{-1}).

The results of thermodynamic parameters are listed in Table 7. The value of ΔG° between 0 and -20 kJ mol^{-1} indicates that it was a natural spontaneous physical adsorption process and that value decreases with the increase of temperature. Meanwhile, the value of $\Delta H^\circ > 0$, indicating that was the endothermic adsorption process. The change of ΔG° and ΔH° with temperature shows that the temperature rise is conducive to this reaction. In binary dye systems, the value ΔH° of MB increases, while the RhB decreases, which may be competitive between MB and RhB increases the difficulty of adsorption, so it takes more heat to adsorb the same amount

Table 4
Isotherm parameters of MB and RhB adsorption on GO/APTG in a single system

Dyes	Model	Parameters	Temperature (K)		
			293	303	313
MB	Langmuir	q_m	409.84	505.05	534.76
		b	0.82	0.75	0.58
		R^2	0.9986	0.9998	0.9988
	Freundlich	R_L	0–0.02	0–0.02	0–0.03
		K_F	191.04	257.49	203.12
		n^{-1}	0.17	0.16	0.24
	Tempkin	R^2	0.6253	0.8743	0.6961
		β	51.32	58.69	73.90
		K_t	26.81	62.72	22.48
	D-R	R^2	0.7002	0.7903	0.7780
		Q_s	378.10	443.35	461.16
		B	7.50×10^{-7}	1.58×10^{-7}	1.58×10^{-7}
	RhB	Langmuir	R^2	0.8867	0.8472
q_m			346.02	363.64	473.93
b			0.10	0.09	0.10
Freundlich		R^2	0.9978	0.9978	0.9966
		R_L	0.03–0.17	0.04–0.18	0.03–0.17
		K_F	87.59	89.14	97.16
Tempkin		n^{-1}	0.27	0.28	0.33
		R^2	0.8729	0.8967	0.8730
		β	61.97	65.31	89.90
D-R		K_t	1.46	1.42	1.32
		R^2	0.8960	0.9148	0.9145
		Q_s	302.07	311.62	389.69
		B	8.08×10^{-6}	6.84×10^{-6}	3.92×10^{-6}
	R^2	0.8570	0.8427	0.8213	

of MB. Moreover, the composite material of GO/APTG has a significantly reduced adsorption capacity for RhB, which reduces the required heat. The positive value of ΔS° , illustrating that the randomness and the affinity were increased in the process of GO/APTG adsorbed dyes.

3.2.7. Removal of different dyes on GO/APTG and reusability of GO/APTG

To further investigate the different removal performances for two different types of dyes on GO/APTG, Fig. 11 shows the removal effect of composite GO/APTG on cationic dyes MB, RhB, BF, CV, and anionic dyes AYR and Orange IV. The results found that the removal efficiencies of cationic dyes (MB, CV, and RhB) using GO/APTG was greater than that of anionic dyes (AYR, Orange IV). This is attributed to the electrostatic attraction that on the surface of GO/APTG is negatively charged. Except for the strong influence of charge of adsorbent on dye adsorption, the structure of cationic dye molecules is also a very important factor. It can be seen clearly in Fig. 11, since the RhB is non-planar molecules hindering the sufficient contact between the adsorbent and the dye, the removal efficiencies don't increase compared to the

anionic dyes. And BF maybe forms macromolecule by intermolecular hydrogen bonds to cause steric hindrance, then to lower the removal efficiency.

Reusability of the GO/APTG composite for the removal of dyes from wastewater is also an important property. In this work, the regeneration of GO/APTG was studied. After adsorbed MB and RhB in the binary system for 60 min, the adsorbents were desorbed by distilled water for 1 h. After five times, the removal capacity of MB and RhB decreased from 237.6, 88.3 to 139.1 mg g⁻¹, 41.2 mg g⁻¹, which implies the strong interactions between dye molecules and adsorbents. The strong forces result in the dyes are not easy to elute, and with the number of cycles increases, the adsorption site on the surface of the GO/APTG is largely occupied, adsorption performance gradual decreases.

3.2.8. Adsorption mechanism

The interaction between the adsorbent and the adsorbate is important in the adsorption process. For carbonaceous materials, the possible interactions identified through research have a hydrophobic effect, π - π bonds stack, hydrogen bonds, and electrostatic interactions, which are the

Table 5
Isotherm parameters of MB and RhB adsorption on GO/APTG in a binary system

Dyes	Model	Parameters	Temperature (K)			
			293	303	313	
MB	Langmuir	q_m	267.37	337.84	534.76	
		b	0.13	0.19	0.58	
		R^2	0.9946	0.9971	0.9988	
	Freundlich	R_L	0.03–0.13	0.02–0.09	0–0.03	
		K_F	140.03	159.88	159.88	
		n^{-1}	0.17	0.16	0.24	
	Tempkin	R^2	0.8728	0.9039	0.9017	
		β	22.59	36.74	43.63	
		K_t	41.94	51.59	31.47	
	D-R	R^2	0.8414	0.9080	0.8593	
		Q_s	237.70	301.46	330.45	
		B	1.93×10^{-7}	2.35×10^{-7}	2.47×10^{-7}	
		R^2	0.6558	0.7746	0.7771	
RhB	Langmuir	q_m	99.50	161.03	168.92	
		b	0.04	0.02	0.02	
		R^2	0.9811	0.9638	0.9699	
	Freundlich	R_L	0.07–0.33	0.14–0.50	0.14–0.50	
		K_F	39.96	20.99	22.59	
		n^{-1}	0.27	0.28	0.33	
	Tempkin	R^2	0.8203	0.9111	0.9075	
		β	11.81	31.35	33.35	
		K_t	8.35	3.99	4.04	
	D-R	R^2	0.7893	0.8827	0.9052	
		Q_s	84.88	113.80	120.78	
		B	3.09×10^{-5}	6.56×10^{-5}	6.33×10^{-5}	
			R^2	0.3675	0.5097	0.5558

Table 6
Adsorption capacities of various adsorbents for MB and RhB in a binary system

	Adsorbent	q_m (mg g ⁻¹)	Adsorption time	Literature
MB	GO/APTG	505.05	250 min	This paper
	APT	192.16	250 min	This paper
	GO-0.1 M NaCl	137.93 ± 4.55	60 h	[30]
	APTES-Fe ₃ O ₄ /bentonite	103.4	200 min	[31]
	MSH	196.00	12 h	[32]
	CA-APT	208.33	400 min	[33]
RhB	GO/APTG	346.02	250 min	This paper
	APT	93.79	250 min	This paper
	MrGO-2	266.5	–	[34]
	Kaolinite	46.08	210 min	[35]
	Sodium montmorillonite	42.19	40 min	[36]

main reason for carbonaceous composite adsorption dyes [37]. However, Tan et al. by reviewing found that the main driving force is the molecular structure, the charge of the dye and electrostatic interactions [38]. The surface of the GO/APTG composite is negatively charged and can easily

adsorb positively charged cationic dyes. By analyzing the experimental data, the rival adsorption is existent between MB and RhB on the surface adsorption sites of GO/APTG, and the MB was distinctly superior to that of RhB. As shown in Fig. 12, in the adsorption process, GO in the composite

Table 7
Thermodynamic parameters of MB and RhB adsorption on GO/APTG

System	Dyes	T/K	ΔG° kJ mol ⁻¹	ΔH° KJ mol ⁻¹	ΔS° J mol ⁻¹ K ⁻¹
Single system	MB	293	-9.024	38.08	161.05
		303	-10.874		
		313	-12.234		
	RhB	293	-4.795	21.04	87.64
		303	-5.169		
		313	-6.570		
Binary system	MB	293	-7.632	50.35	197.91
		303	-9.643		
		313	-11.589		
	RhB	293	-0.004	4.54	15.45
		303	-0.105		
		313	-0.311		

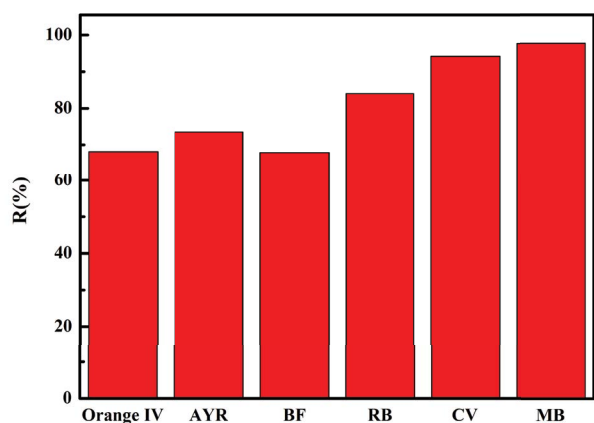


Fig. 11. GO/APTG removal effect on different dyes.

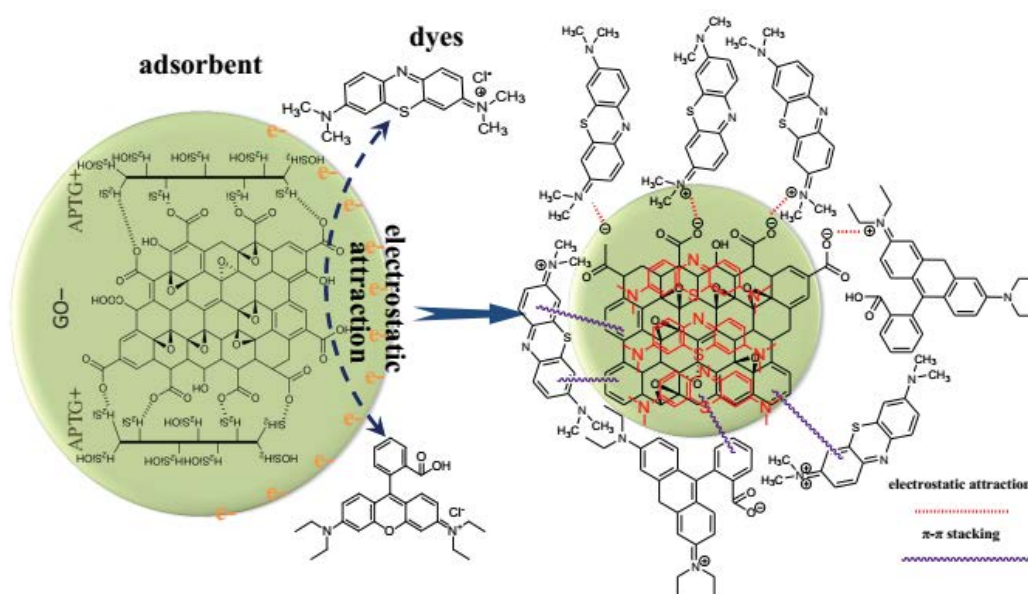


Fig. 12. Mechanism schematic diagram of MB (a) and RhB (b) adsorption on GO/APTG.

material plays a major adsorption role. Besides electrostatic force, there is π - π bonds stack interaction between GO and dyes. MB with the planar molecular structure to favor the π - π interaction between GO and MB, which causes GO has a higher affinity to MB. And the RhB has a non-planar molecule structure and the relatively large molecular weight, which increases the difficulty of adsorption. Additionally, the adsorption effect of APTG on MB is also better than RhB. Therefore, MB occupies a large number of adsorption sites in the binary dye, and forms a steric hindrance to RhB, at the same time, which inhibits the adsorption of RhB on the GO/APTG composite. The results suggest that electrostatic attractions and π - π interaction play essential roles. Additionally, the molecule structure of dye exerts a certain influence on the removal process. This is consistent with the result of adsorption.

4. Conclusion

The modified APTG was uniformly attached to the surface of GO to form the composite GO/APTG by the electrostatic interaction between GO and APTG. After combined with APT, the GO/APTG possess high adsorption performances for cationic dyes, especially when the quality ratio of GO to APTG is 1:1, the maximum experiment adsorption capacity of MB and RhB reach 534.76 and 473.93 mg g⁻¹, respectively in single-dye solution. And there is a rival adsorption in binary-dye systems, compared to RhB, MB more preferentially adsorbed on the GO/APTG. Additionally, the adsorption process conforms to the Langmuir model and pseudo-second-order kinetics in single or binary dye solutions, suggesting monolayer and chemical adsorption. Removal mechanism suggests that electrostatic attractions and π - π stacking play essential roles. And the structures of dyes molecules exert a certain influence on the removal process. It was confirmed by experiments that the synthesized adsorptions GO/APTG has good adsorption performance for cationic dyes, which not only reduces the cost of GO but also makes good use of the perfect adsorption performance of APTG. However, in this system, the reusability of the GO/APTG composite is not satisfied which needs to be further improved, and recycling of adsorbed products, the adsorbents accumulation after adsorption dyes tends to cause secondary pollution, will be discussed in the following work (Such as fabricating electrode material through calcination approach).

Acknowledgments

This work was supported by the National Natural Science Foundations of China (51763015, 51503092), Lanzhou University of technology HongLiu first-class discipline construction program and the Foundation for Innovation Groups of Basic Research in Gansu Province (No. 1606RJIA322).

References

- G.Z. Kyzas, N.K. Lazaridis, M. Kostoglou, On the simultaneous adsorption of a reactive dye and hexavalent chromium from aqueous solutions onto grafted chitosan, *J. Colloid Interface Sci.*, 407 (2013) 432–441.
- X.Y. Jin, Z.X. Chen, R.B. Zhou, Z.L. Chen, Synthesis of kaolin supported nanoscale zero-valent iron and its degradation mechanism of Direct Fast Black G in aqueous solution, *Mater. Res. Bull.*, 61 (2015) 433–438.
- Z.X. Chen, T. Wang, X.Y. Jin, Z.L. Chen, M. Megharaj, R. Naidu, Multifunctional kaolinite-supported nanoscale zero-valent iron used for the adsorption and degradation of crystal violet in aqueous solution, *J. Colloid Interface Sci.*, 398 (2013) 59–66.
- S.E. Shaibu, F.A. Adekola, H.I. Adegoke, O.S. Ayanda, A comparative study of the adsorption of methylene blue onto synthesized nanoscale zero-valent iron-bamboo and manganese-bamboo composites, *Materials*, 7 (2014) 4493–4507.
- T.H. Liu, Y.H. Li, Q.J. Du, J.K. Sun, Y.Q. Jiao, G.M. Yang, Z.H. Wang, Y.Z. Xia, W. Zhang, K.L. Wang, H.W. Zhu, D.H. Wu, Adsorption of methylene blue from aqueous solution by graphene, *Colloids Surf., B*, 90 (2012) 197–203.
- J.Y. Chen, Y.M. Hao, Y. Liu, J.J. Gou, Magnetic graphene oxides as highly effective adsorbents for rapid removal of a cationic dye rhodamine B from aqueous solutions, *RSC Adv.*, 3 (2013) 7254–7258.
- A.G. Akerdi, Z. Es'haghzade, S.H. Bahrami, M. Arami, Comparative study of GO and reduced GO coated graphite electrodes for decolorization of acidic and basic dyes from aqueous solutions through heterogeneous electro-Fenton process, *J. Environ. Chem. Eng.*, 5 (2017) 2313–2324.
- Y.S. Wang, Z. Li, X.F. Ren, H. Song, A.Q. Wang, Removal of Methyl Violet from aqueous solutions using poly (acrylic acid-co-acrylamide)/attapulgite composite, *J. Environ. Sci.*, 22 (2010) 7–14.
- A.L. Xue, S.Y. Zhou, Y.J. Zhao, X.P. Lu, P.F. Han, Effective NH₂-grafting on attapulgite surfaces for adsorption of reactive dyes, *J. Environ. Sci.*, 194 (2011) 7–14.
- H.L. Lu, H. Xu, Y. Chen, J.L. Zhang, J.X. Zhuang, ZVI/PANI/ATP composite by static polymerization as adsorbent for removal of Cr(VI), *RSC Adv.*, 4 (2014) 5873–5879.
- W.B. Wang, A.Q. Wang, Recent progress in dispersion of palygorskite crystal bundles for nanocomposites, *Appl. Clay Sci.*, 119 (2016) 18–30.
- H. Xu, Y. Xu, Y. Chen, Adsorption of eriochrome blue black on polyaniline/attapulgite nanocomposites, *Adv. Mater. Res.*, 194–196 (2011) 488–491.
- B. Mu, A.Q. Wang, Adsorption of dyes onto palygorskite and its composites: a review, *J. Environ. Chem. Eng.*, 4 (2016) 1274–1294.
- G. Ersan, G.A. Onur, F. Perreault, T. Karanfil, Adsorption of organic contaminants by graphene nanosheets: a review, *Water Res.*, 126 (2017) 385–398.
- G.-P. Salvador, P. Roquero, B.-G. Mauricio, Z.-F. Daniel, Study of structural defects on reduced graphite oxide generated by different reductants, *Diamond Relat. Mater.*, 92 (2019) 219–227.
- W.S. Hummers Jr., R.E. Offeman, Preparation of graphitic oxide, *J. Am. Chem. Soc.*, 80 (1958) 1339–1339.
- S.B. Wang, C. Wei Ng, W.T. Wang, Q. Li, Z.P. Hao, Synergistic and competitive adsorption of organic dyes on multiwalled carbon nanotubes, *Chem. Eng. J.*, 197 (2012) 34–40.
- Q. Meng, Z. Shi, S. Wang, Attapulgite surface modification and its application in the wastewater treatment, *J. Chin. Ceram. Soc.*, 27 (2008) 996–999.
- Y.H. Liu, X.Q. Jiang, B.J. Li, X.D. Zhang, T.Z. Liu, X.S. Yan, J. Ding, Q. Cai, J.M. Zhang, Halloysite nanotubes@reduced graphene oxide composite for removal of dyes from water and as supercapacitors, *J. Mater. Chem.*, 2 (2014) 4264–4269.
- M. Kumar, H.S. Dosanjh, H. Singh, Magnetic zinc ferrite-chitosan bio-composite: synthesis, characterization and adsorption behavior studies for cationic dyes in single and binary systems, *J. Inorg. Organomet. Polym. Mater.*, 28 (2018) 880–898.
- S. Hu, Comparison on modification effect on attapulgite by CTAB and KH550, *Mon-Met. Mines.*, 6 (2009) 50–52.
- A. Singh, A. Chandra, Graphite oxide/polypyrrole composite electrodes for achieving high energy density supercapacitors, *J. Appl. Electrochem.*, 43 (2013) 773–782.
- S. Stanly, E.J. Jelmy, C.P.R. Nair, H. John, Carbon dioxide adsorption studies on modified montmorillonite clay/reduced graphene oxide hybrids at low pressure, *J. Environ. Chem. Eng.*, 7 (2019) 103344.
- M. Bahgat, A.A. Farghali, W. El Roubi, M. Khedr, M.Y. Mohassab-Ahmed, Adsorption of methyl green dye onto multi-walled carbon nanotubes decorated with Ni nanoferrite, *Appl. Nanosci.*, 3 (2013) 251–261.
- X.L. Weng, Z. Lin, X.F. Xiao, C.Y. Li, Z.L. Chen, One-step biosynthesis of hybrid reduced graphene oxide/iron-based nanoparticles by *eucalyptus* extract and its removal of dye, *J. Cleaner Prod.*, 203 (2018) 22–29.
- Z.-L. Cheng, Y.-X. Li, Z. Liu, Novel adsorption materials based on graphene oxide/Beta zeolite composite materials and their adsorption performance for rhodamine B, *J. Alloys Compd.*, 708 (2017) 255–263.
- I.M. Reck, R.M. Paixao, R. Bergamasco, M.F. Vieira, A.M.S. Vieira, Removal of tartrazine from aqueous solutions using adsorbents based on activated carbon and *Moringa oleifera* seeds, *J. Cleaner Prod.*, 171 (2018) 85–97.
- R. Xi, G.Y. Cédric, O. Stephanie, D.S. Bradley, C.L. Chu, T. Michaël, A.H. Ali, High density gold nanoparticles immobilized on surface via plasma deposited APTES film for

- decomposing organic compounds in microchannels, *Appl. Surf. Sci.*, 439 (2018) 272–281.
- [29] G.K. Ramesh, A.V. Kumar, H.B. Muralidhara, S. Sampath, Graphene and graphene oxide as effective adsorbents toward anionic and cationic dyes, *J. Colloid Interface Sci.*, 361 (2011) 270–277.
- [30] A. Ojha, P. Thareja, Electrolyte induced rheological modulation of graphene oxide suspensions and its applications in adsorption, *Appl. Surf. Sci.*, 435 (2018) 786–798.
- [31] Z.C. Lou, W. Zhang, X.D. Hu, H.Q. Zhang, Synthesis of a novel functional group-bridged magnetized bentonite adsorbent: characterization, kinetics, isotherm, thermodynamics and regeneration, *Chin. J. Chem. Eng.*, 25 (2017) 587–594.
- [32] R.R. Pawar, Lalhmunsiam, P. Gupta, Y.S. Sawant, B. Shahmoradi, S.M. Lee, Porous synthetic hectorite clay-alginate composite beads for effective adsorption of methylene blue dye from aqueous solution, *Int. J. Biol. Macromol.*, 114 (2018) 1315–1324.
- [33] Z.F. Zhang, W.B. Wang, A.Q. Wang, Highly effective removal of Methylene Blue using functionalized attapulgite via hydrothermal process, *J. Environ. Sci.*, 33 (2015) 106–115.
- [34] M. Neelaveni, P.S. Krishnan, R. Ramya, G. Sonia Theres, K. Shanthi, Montmorillonite/graphene oxide nanocomposite as superior adsorbent for the adsorption of Rhodamine B and Nickel ion in binary system, *Adv. Powder. Technol.*, 30 (2019) 596–609.
- [35] T.A. Khan, S. Dahiya, I. Ali, Use of kaolinite as adsorbent: equilibrium, dynamics and thermodynamic studies on the adsorption of Rhodamine B from aqueous solution, *Appl. Clay Sci.*, 69 (2012) 58–66.
- [36] P.P. Selvam, S. Preethi, P. Basakaralingam, N.X. Thinakaran, A. Sivasamy, S. Sivanesan, Removal of rhodamine B from aqueous solution by adsorption onto sodium montmorillonite, *J. Hazard. Mater.*, 155 (2008) 39–44.
- [37] M. Kah, G. Sigmund, F. Xiao, T. Hofmann, Sorption of ionizable and ionic organic compounds to biochar, activated carbon and other carbonaceous materials, *Water Res.*, 124 (2017) 673–692.
- [38] K.B. Tan, M. Vakili, B.A. Horri, P.E. Poh, A.Z. Abdullah, B. Salamatinia, Adsorption of dyes by nanomaterials: recent developments and adsorption mechanisms, *Sep. Purif. Technol.*, 150 (2015) 229–242.